VOLUME 111, NUMBER 26
DECEMBER 20, 1989

JOURNAL
OF THE
AMERICAN
CHEMICAL
SOCIETY

UV Resonance Raman Enhancement of Vinyl Stretching in Ferric Protoporphyrin IX: Conjugation and Preservation of the Vinyl $\pi \rightarrow \pi^*$ Transition

Valentino L. DeVito and Sanford A. Asher*

Contribution from the Department of Chemistry, University of Pittsburgh, Pittsburgh, Pennsylvania 15260. *Received November 3, 1988*

Abstract: The resonance Raman spectra of ferric protoporphyrin IX (PP) complexes show selective vinyl enhancement with UV excitation below 300 nm. These complexes include the five-coordinate high-spin μ-oxo dimer $[Fe(PP)]_2O$, and the six-coordinate low-spin bisliganded porphyrin complexes of imidazole (ImH) and cyanide, $[(ImH)_2Fe(PP)]^+$ and $[(CN)_2Fe(PP)]^-$. Excitation in the 220–275-nm region results in selective enhancement of both the vinyl C=C stretching mode(s) at 1622 cm^{-1} and the vinyl–heme stretch(es) at 1125 cm^{-1} in $[(CN)_2FePP)]^-$. In contrast, the μ-oxo and bis(imidazole) complexes show selective enhancement of only the 1622-cm^{-1} mode. This vinyl mode enhancement derives from an electronic transition at ca. 200 nm, which appears to be an almost isolated vinyl $\pi \rightarrow \pi^*$ transition. We have compared vinyl group Raman enhancement of PP complexes in the Soret band and in the UV and have also examined the C=C enhancement in 1-hexene and 1,3-hexadiene. We conclude that little conjugation occurs between the vinyl groups and the porphyrin ring in the ground electronic state. In contrast, resonance enhancement of the vinyl vibrational modes with visible Soret excitation occurs because of a small amount of conjugation between the vinyl π^* antibonding orbitals and the porphyrin excited π^* Soret orbitals. We definitively assign a new relatively isolated vinyl electronic transition in the UV absorption spectrum of protoporphyrin IX at ca. 200 nm.

Metalloporphyrins are ubiquitous in nature as prosthetic groups in proteins such as hemoglobin and the cytochromes. The most common porphyrin in nature, protoporphyrin IX (PP), contains two vinyl substituents, which are generally thought to be completely conjugated with the porphyrin ring, thus forming a single delocalized π system.[1] It has been suggested that these vinyl groups serve an important role in a scheme where the protein exercises steric control over the vinyl orientations which, in turn, control the ligand binding and redox properties.[2-7] Related to this mechanism, several workers have speculated that the electron-withdrawing effects of the vinyl groups on the porphyrin π-electron density might strongly influence the ligand binding affinity of the protein.[3,4] Desbois and co-workers attempted to correlate the frequencies of several Raman bands involving vinyl deformation modes with protein–vinyl conformation as determined from X-ray crystallographic data.[8] In fact, no definitive evidence as yet exists to demonstrate the enzymatic role of the heme vinyl groups. Possibly, the assumption of extensive vinyl conjugation is incorrect. This is supported by recent structural studies showing that, in the ground state, the vinyl groups are oriented out of the plane of the porphyrin ring by an angle of $\sim 50°$ and by the theoretical studies that conclude a lack of ground-state vinyl conjugation.[9-15]

(1) Gouterman, M. In *The Porphyrins*; Dolphin, D., Ed.; Academic Press: New York, 1978; Vol. III, pp 1–165.
(2) Alben, J. O.; Caughey, W. S. *Biochemistry* **1968**, *7*, 175–183.
(3) (a) Asakura, T.; Sono, M. *J. Biol. Chem.* **1974**, *249*, 7087–7093. (b) Sono, M.; Asakura, T. *J. Biol. Chem.* **1975**, *250*, 5227–5232.
(4) Warshel, A.; Weiss, R. M. *J. Am. Chem. Soc.* **1981**, *103*, 446–451.
(5) Rousseau, D. L.; Ondrias, M. R.; LaMar, G. N.; Kong, S. B.; Smith, K. M. *J. Biol. Chem.* **1983**, *258*, 1740–1746.
(6) Gelin, B. R.; Karplus, M. *Proc. Natl. Acad. Sci. U.S.A.* **1977**, *74*, 801–805.
(7) Reid, L. S.; Lim, A. R.; Mauk, A. G. *J. Am. Chem. Soc.* **1986**, *108*, 8197–8201.
(8) Desbois, A.; Mazza, G.; Stetzkowski, F.; Lutz, M. *Biochim. Biophys. Acta* **1984**, *785*, 161–176.

0002-7863/89/1511-9143$01.50/0

Resonance Raman (RR) spectroscopy has proven to be a powerful probe of porphyrin structure.[16] Numerous visible-wavelength Raman excitation studies in the α, β, CT, and Soret bands have carefully characterized the porphyrin vibrational modes. Several different high-frequency, in-plane porphyrin skeletal modes are typically used as markers for metal oxidation state, spin state, coordination number, and porphyrin core size.[16] In addition to characterizing the ground-state prophyrin structure, Raman spectroscopy can also probe excited-state structure and dynamics; resonance Raman excitation profiles are powerful tools for the assignment of electronic transitions.[17]

In this work we examine the resonance Raman spectra of iron(III) μ-oxo dimer, the bis(cyanide) and the bis(imidazole) complexes of protoporphyrin IX in aqueous solution at excitations between 220 and 300 nm. We unexpectedly find that the only vibrational modes exhibiting selective enhancement with UV excitation are the 1125-cm^{-1} vinyl–heme stretch(es) and the 1622-cm^{-1} symmetric vinyl C=C stretch(es) of the bis(cyanide) complex. A similar enhancement limited to the 1622-cm^{-1} vinyl stretch occurs for the bis(imidazole) and μ-oxo complexes. The other porphyrin vibrational modes show relatively weak enhancements. These results, as well as previously observed strong vinyl enhancement with Soret excitation, compel us to reexamine the conventional wisdom concerning vinyl group π conjugation with the porphyrin ring. The excitation profiles allow us to assign, for the first time, a porphyrin electronic transition in the UV. We also establish here a new and powerful method to address the important question of the role of vinyl groups in heme protein function.

Experimental Section

Samples of the iron(III) protoporphyrin IX (hemin) complexes were prepared in the following manner. Hemin (bovine; Aldrich Chemical Co., Milwaukee, WI) was used without further purification and was dissolved in doubly distilled, deionized water that had been adjusted to a pH of 9 by addition of 1 M sodium hydroxide (Fisher Scientific). This resulted in a green solution of the μ-oxo dimer. The solution turned deep red upon addition of a 30-fold molar excess of either sodium cyanide (Aldrich) or imidazole (Sigma Chemical Co., St. Louis, MO). The NaCN was used as received and the imidazole was purified by sublimation prior to use. The dimethyl ester of iron(III) protoporphyrin IX was prepared from hemin in a 5% H_2SO_4–CH_3OH solution at −10 °C by using the methods described by Falk.[18] The dichloromethane (Mallinckrodt, St. Louis, MO) was refluxed with P_2O_5, distilled, and stored over 4-Å molecular sieves. Solution concentrations for the Raman measurements ranged from 0.8 to 1.0 mM in porphyrin. Sodium perchlorate (Aldrich) was used as an internal standard at concentrations of 0.5 M. Absorption spectra were measured by using an IBM Model 9420 UV–visible spectrophotometer.

The samples were circulated through a jet nozzle by a magnetic gear pump and changed after each 15-min scan. Absorption spectra run immediately after removing the samples from the laser beam showed no indication of photodegradation. The Raman spectrometer has been described in detail elsewhere.[19] The excitation source is a Quanta-Ray DCR-2A Nd–YAG laser operated at 20 Hz, whose output is frequency doubled to pump a dye laser. The 275-nm radiation was generated via frequency doubling of the output of the dye laser (fluorescein 548). Excitation at 250 nm and below was generated by mixing the doubled dye output with the laser 1.06-μm YAG fundamental. The photon energy flux incident upon the sample ranged from about 5 to 20 mJ/(cm^2·pulse). An ellipsoidal mirror collected the scattered light at 90° from the incident beam and a polarization scrambler was utilized to avoid any polarization bias of the instrument. The depolarization ratios, ρ, were measured by placing a Polacoat analyzer in front of the polarization scrambler. As a test for determinate errors due to "leakage" of unwanted polarizations through the polarizer (either because of the large solid angle collected or because of incomplete extinction), we measured the depolarization ratio of CCl_4 excited at 488 nm and obtained ratios of 0.06 and 0.73 for the 459- and 218-cm^{-1} bands, respectively. The literature values[20] for these modes are 0.02 and 0.75, respectively. The large relative error in the polarized band derives mainly from the transmission of 4% residual parallel polarization in the perpendicular polarization measurement. At higher depolarization ratios, the relative error is much smaller with ca. 7% and 3% errors for ρ = 0.45 and 0.75 measurements. For the 932-cm^{-1} perchlorate band with 222-nm excitation we obtained a depolarization ratio of 0.08, which is somewhat greater than expected for this symmetric molecule. Assuming a similar transmittance of the UV parallel polarized radiation for the perpendicular polarization measurement we obtain similar error limits for the UV depolarization ratios as for the visible spectral region. A Spex Triplemate monochromator equipped with a Model 1420 blue-enhanced intensified Reticon detector dispersed and detected the scattered light, and spectra were accumulated on a Princeton Applied Research OMA II computer.

The throughput efficiency of the monochromator in the UV was determined with a standard intensity lamp. Total Raman cross sections (cm^2/sr·molecule) were calculated from the measured peak areas of the bands relative to $NaClO_4$ by the methods outlined by Dudik et al.[21] Due to the narrow stream diameter (0.25 mm) of the jet, self-absorption was negligible. The reported frequencies are accurate to within ±5 cm^{-1}. The relative standard deviation of the reported Raman cross sections of the μ-oxo dimer and the bis(cyanide) hemin adduct are estimated to be accurate to within 20%, mainly due to uncertainties in the standard band cross sections. We estimate larger possible errors in the bis(imidazole) hemin adduct due to the strong interferences from the Raman scattering of the excess free imidazole in solution. Interference from free imidazole increased as the excitation wavelength decreased, such that the 220-nm spectrum shows only Raman bands from imidazole.

The olefin model compounds 1-hexene and 1,3-hexadiene (Aldrich) were used as received and prepared as dilute solutions in acetonitrile. Their Raman spectra were measured under conditions identical with those for the porphyrin samples except that a 1.0-mm-i.d. suprasil quartz capillary replaced the jet nozzle. Total Raman cross sections were calculated relative to the acetonitrile 918-cm^{-1} mode.[21]

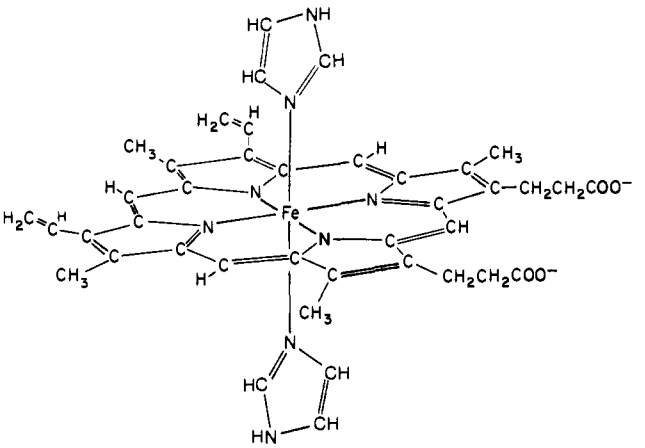

Figure 1. Structure of bis(imidazole) iron(III) protoporphyrin IX at pH 9.

(9) Bothner-By, A. A.; Gayathri, C.; van Zijl, P. C. M.; MacLean, C.; Lai, J.; Smith, K. M. *Magn. Reson. Chem.* **1985**, *23*, 935–938.
(10) LaMar, G. N.; Viscio, D. B.; Gersonde, K.; Sick, H. *Biochemistry* **1978**, *17*, 361–367.
(11) LaMar, G. N. Burns, P. D.; Jackson, J. T.; Smith, K. M.; Langry, K. C.; Strittmatter, P. *J. Biol. Chem.* **1981**, *256*, 6075–6079.
(12) Thanabal, V.; deRopp, J. S.; LaMar, G. N. *J. Am. Chem. Soc.* **1986**, *108*, 4244–4245.
(13) Little, R. G.; Dymock, K. R.; Ibers, J. A. *J. Am. Chem. Soc.* **1975**, *97*, 4532–4539.
(14) Caughey, W. S.; Ibers, J. A. *J. Am. Chem. Soc.* **1977**, *99*, 6639–6645.
(15) Findsen, L. A.; Bocian, D. F.; Birge, R. R. *J. Chem. Phys.* **1988**, *88*, 7588–7598.
(16) For reviews, see: (a) Kitagawa, T.; Ozaki, Y. *Structure and Bonding*; Springer-Verlag: Berlin, 1987; pp 71–114. (b) Yu, N. T. *Methods Enzymol.* **1986**, *130*, 350–409. (c) Sprio, T. G. *Adv. Protein Chem.* **1985**, *37*, 111–159. (d) Spiro, T. G. In *Iron Porphyrins, Part III*; Lever, A. B. P., Gray, H. B., Eds.; Addison-Wesley Publishing Co.: Reading, MA, 1983; pp 89–159. (e) Asher, S. A. *Methods Enzymol.* **1981**, *76*, 371–413. (f) Kitagawa, T.; Ozaki, Y.; Kyogoku, Y. *Adv. Biophys.* **1978**, *11*, 153–196. (g) Felton, R. H.; Yu, N. T. In *The Porphyrins*; Dolphin, D., Ed.; Academic Press: New York, 1978; Vol. III, pp 347–393. (h) Sprio, T. G. *Biochim. Biophys. Acta* **1975**, *416*, 169–189.
(17) Asher, S. A. *Annu. Rev. Phys. Chem.* **1988**, *39*, 537–588.
(18) Falk, J. E. *Porphyrins and Metalloporphyrins*; Elsevier: Amsterdam, 1964; pp 125–127.
(19) (a) Asher, S. A.; Johnson, C. R.; Murtaugh, J. L. *Rev. Sci. Instrum.* **1983**, *54*, 1657–1662. (b) Asher, S. A. *Appl. Spectrosc.* **1984**, *38*, 276–278.
(20) Nakamoto, K. *Infrared and Raman Spectra of Inorganic and Coordination Compounds*, 4th ed.; Wiley: New York, 1986; p 74.
(21) Dudik, J. M.; Johnson, C. R.; Asher, S. A. *J. Chem. Phys.* **1985**, *82*, 1732–1740.

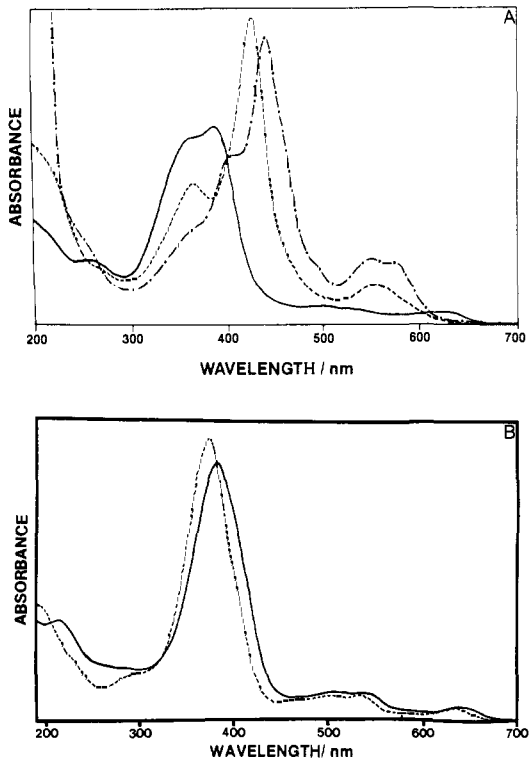

Figure 2. (A) Absorption spectra of aqueous solutions of μ-oxo hemin dimer (—), bis(cyanide) hemin (---), and bis(imidazole) hemin (-·-) at pH 9. The concentration of the μ-oxo hemin dimer is 0.25 mM while the bisliganded hemin concentrations are 0.50 mM. Path length is 0.05 cm. The CN^- and ImH ligands are added in a 30-fold molar excess. (B) Absorption spectra of Fe(III) octaethylporphyrin chloride (---) and Fe(III) protoporphyrin IX dimethyl ester chloride (—) in acetonitrile. Porphyrin concentrations are 3.0×10^{-5} M. Pathlength is 0.5 cm.

Results

Figure 1 shows the structure of the bis(imidazole) iron(III) protoporphyrin IX complex. This porphyrin, known as heme, has a variety of substituents, including two vinyl groups, two propionic acid groups, and four methyl substituents. Figure 2A shows the electronic absorption spectra of the three hemin complexes prepared as aqueous solutions at pH 9. The green μ-oxo hemin dimer, $[(PP)Fe^{III}]_2O$, a five-coordinate high-spin complex, gives rise to a weak band at 630 nm, Q bands at 530 and 494 nm, split Soret (B) absorption bands at 385 and 368 nm, a weak band at 262 nm, and a shoulder at ca. 210 nm. The red bis(imidazole) hemin adduct, $[(ImH)_2Fe^{III}(PP)]^+$, a six-coordinate low-spin compound, has its Q bands at 566 and 542 nm, split Soret bands at 436 and 402 nm, and shoulders at 368 and 262 nm. The strong absorption below 240 nm derives from the excess free imidazole required to ensure bis-complexation. The bis(imidazole) hemin spectrum shown in Figure 2A is identical with that reported by Mitchell et al.[22] obtained at pH 10. The red bis(cyanide) hemin adduct, $[(CN)_2Fe^{III}(PP)]^-$, which is a six-coordinate low-spin complex, shows a single Q band centered at 546 nm, a Soret band at 422 nm, a relatively strong band at 364 nm, and a weak shoulder at 262 nm. In addition, a pronounced shoulder at ca. 212 nm lies on the far-UV peak. The spectrum of the bis(cyanide) hemin derivative in water appears identical with that in DMF reported by Lukas and Silver[23] and Scheidt et al.[24]

Split Soret features as observed for the μ-oxo dimer and bis(imidazole) species presumably derive from molecular aggregation.[22] Gouterman and co-workers reported that the spectra of μ-oxo dimers of scandium(III) porphyrins exhibit large blue shifts and Soret band splitting compared with the monomeric complexes and suggested that these spectral differences derive from exciton coupling between the porphyrin rings in the dimer.[25]

The absorption shoulders at 262 nm common to all three porphyrins (but strongest for the μ-oxo complex) probably correspond to the "extra" $\pi \rightarrow \pi^*$ band (L) discussed by Edwards et al. in their gas-phase absorption studies of metal octaalkylporphyrins.[26] The ca. 365-nm transition found for the bis(cyanide) and bis(imidazole) adducts probably derives from a higher lying porphyrin $\pi \rightarrow \pi^*$ transition (N) as assigned by various workers.[26,27] Addition of excess cyanide or imidazole forms the bis-adducts, and for cyanide, the split Soret band narrows to a single band. The bis(imidazole) complex, in contrast, retains a split Soret with an additional peak at 402 nm, which may be indicative of aggregation.[22] Possibly hydrogen bonding plays a significant role in the aggregate formation.[22,28,29] Our Raman data (vide infra) are in full agreement with the results of Choi et al.,[30] who found that aggregation had little effect on the vibrational band frequencies.

$NaClO_4$ was added to the porphyrin solutions in large excess as an internal intensity standard. Since no absorption spectral changes were observed, $NaClO_4$ addition did not affect the equilibria for the μ-oxo and bis(cyanide) complexes. For the bis(imidazole) spectrum, addition of the $NaClO_4$ caused an increase in the relative intensity of the 402-nm shoulder, but without a wavelength shift. Though the predominant species definitely remains the biscomplex, the high salt concentration may disturb the aggregate structure. Although we do not clearly understand the effect of the perchlorate on porphyrin aggregation, we find that addition of $NaClO_4$ negligibly affects the Raman frequencies and cross sections.

The entire near-UV region of porphyrin absorption from 200 to 260 nm is very broad and featureless with bands of moderate molar absorptivity that extend further into the vacuum-UV. The molar absorptivities measured at 220 nm for the μ-oxo dimer and the bis(cyanide) hemin complexes are 5.1×10^4 and 4.3×10^4 M^{-1} cm^{-1}, respectively. These values are roughly half that at the maxima of the respective Soret transitions for these complexes. Due to the strong absorbance of the excess free imidazole, the molar absorptivity of the bis(imidazole) hemin adduct could not be determined below 240 nm. Although the UV bands below 300 nm are not clearly assignable to any particular transitions, it is likely that they involve porphyrin $\pi \rightarrow \pi^*$ transitions.[1,31] To our knowledge no detailed description of these higher lying π,π^* states exists.[1,32-34]

Figure 2B compares the absorption spectra of the chloride complexes of ferric octaethylporphyrin (Fe(OEP)Cl) and ferric protoporphyrin IX dimethyl ester (Fe(PP-DME)Cl) in acetonitrile. The more complex substitution pattern of the protoporphyrin IX derivative does not dramatically modify the visible and near-UV absorption spectrum since the Soret and Q bands show very similar patterns. The ca. 10-nm red shift for Fe(PP-DME)Cl is assumed to derive mainly from the vinyl functional groups. A larger absorption spectral difference is evident in the UV, where the PP derivative shows a new weak band at ca. 215 nm (ϵ = 33000 M^{-1} cm^{-1}) compared to Fe(OEP)Cl (ϵ = 26000 M^{-1} cm^{-1}). In ad-

(22) Mitchell, M. L.; Li, X. Y.; Kincaid, J. R.; Spiro, T. G. *J. Phys. Chem.* **1987**, *91*, 4690-4696.
(23) Lukas, B.; Silver, J. *Inorg. Chim. Acta* **1986**, *124*, 97-100.
(24) Scheidt, W. R.; Haller, K. J.; Hatano, K. *J. Am. Chem. Soc.* **1980**, *102*, 3017-3021.
(25) Gouterman, M.; Holtan, D.; Lieberman, E. *Chem. Phys.* **1977**, *25*, 139-153.
(26) Edwards, L.; Dolphin, D.; Gouterman, M. *J. Mol. Spectrosc.* **1970**, *35*, 90-109.
(27) (a) Makinen, M. W.; Eaton, W. A. *Ann. N. Y. Acad. Sci.* **1973**, *206*, 210-222. (b) Eaton, W. A.; Hofrichter, J. *Methods Enzymol.* **1981**, *76*, 175-261.
(28) Sundberg, R. J.; Martin, R. B. *Chem. Rev.* **1974**, *74*, 471-517.
(29) Matuszak, C. A.; Matuszak, A. J. *J. Chem. Educ.* **1976**, *53*, 280-284.
(30) Choi, S.; Spiro, T. G.; Langry, K. C.; Smith, K. M.; Budd, D. L.; LaMar, G. N. *J. Am. Chem. Soc.* **1982**, *104*, 4345-4351.
(31) (a) Seno, Y.; Otsuka, J. *Adv. Biophys.* **1978**, *11*, 13-49. (b) Adar, F. *The Porphyrins*; Dolphin, D., Ed.; Academic Press: New York, 1978; Vol. III, pp 167-209.
(32) Chantrell, S. J.; McAuliffe, C. A.; Munn, R. W.; Pratt, A. C. *Coord. Chem. Rev.* **1975**, *16*, 259-284.
(33) Zerner, M.; Gouterman, M. *Theor. Chim. Acta* **1966**, *4*, 44-63.
(34) Zerner, M.; Gouterman, M.; Kobayashi, H. *Theor. Chim. Acta* **1966**, *6*, 363-400.

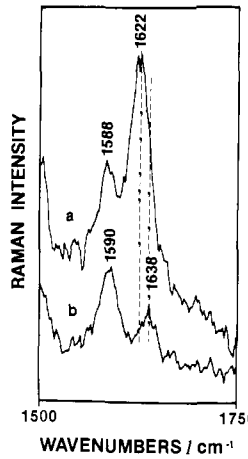

Figure 3. Raman difference spectra of (a) $[(ImH)_2Fe(PP\text{-}DME)]^+$ and (b) $[(ImH)_2Fe(OEP)]^+$ in CH_2Cl_2 excited with 275-nm radiation. The porphyrin concentration is 0.8 mM.

dition, the molar absorptivities of the PP derivative are larger than those of the OEP derivative everywhere between 210 and 300 nm. The relevent questions are what role does the vinyl play in these absorption spectral differences and how are the frontier orbitals of the vinyl substituents mixed with the heme ring? What are the assignments of these UV heme electronic transitions? Further, a comparison between parts A and B of Figure 2 indicates a large solvent dependency of the UV absorption spectrum. Does the local heme environment determine the nature of the heme UV electronic transitions?

Figure 3 shows the 275-nm excited Raman spectra of the bis(imidazole) complexes of ferric protoporphyrin IX dimethyl ester and ferric octaethylporphyrin dissolved in CH_2Cl_2. We were unable to obtain spectra at shorter wavelengths due to the CH_2Cl_2 solvent absorption, and because the poor solubility of Fe(OEP)Cl severely limits our choice of solvent. We used the dimethyl ester of protoporphyrin IX because of its high solubility in dichloromethane. $[(ImH)_2Fe^{III}(PP\text{-}DME)]^+$ gives rise to two major peaks at 1588 and 1622 cm^{-1}. $[(ImH)_2Fe^{III}(OEP)]^+$ yields a slightly higher frequency peak at 1590 cm^{-1} but the strong 1622-cm^{-1} band is absent and only a far weaker intensity band at 1638 cm^{-1} is observed. On the basis of the unique enhancement of the 1622-cm^{-1} band in the protoporphyrin complex and the previous definitive assignments of vinyl stretching modes at ca. 1620 cm^{-1} with Soret excitation, we conclude that the intense band at 1622 cm^{-1} involves primarily vinyl symmetric stretching.[30,35-37] The 1588- and 1590-cm^{-1} bands are easily assigned to the ν_2 in-plane porphyrin symmetric pyrrole stretch, C_bC_b.[16,38] The 1638-cm^{-1} peak clearly derives from the asymmetric ν_{10} in-plane porphyrin methine–pyrrole C_aC_m stretching mode by analogy to the work of Teraoka and Kitagawa.[39] The assignments are based on the normal mode calculations of Abe et al.[40,41] The ν_{10} band in the protoporphyrin IX species is hidden under the much greater intensity mode at 1622 cm^{-1}.

Figure 4, which shows Raman spectra of the three porphyrin complexes excited at 225, 250, and 275 nm, demonstrates that the 1622-cm^{-1} vinyl stretching mode dominates the UV Raman spectra in contrast to its relatively weak enhancement with visible-wavelength Soret and Q band excitation. In addition, we also observe a selective enhancement for a ca. 1125-cm^{-1} band that

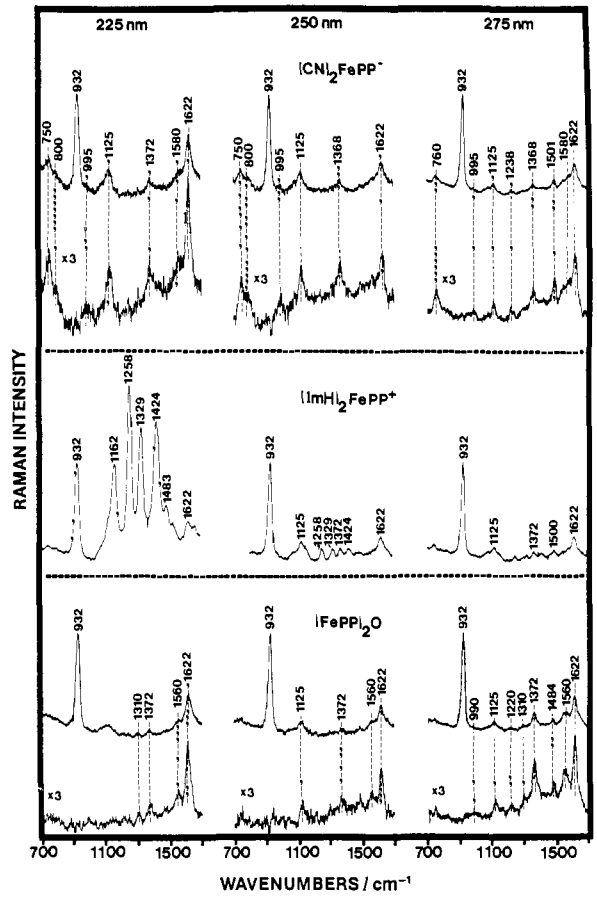

Figure 4. Raman spectra of hemin complexes in aqueous solution at pH 9. The mode at 932 cm^{-1} derives from the $NaClO_4$ internal standard. The internal standard and porphyrin concentrations are 500 and 1.0 mM, respectively. The difference spectra displayed for the bis(cyanide) and μ-oxo complexes derive from replicate measurements in which the contributions from the water and ClO_4^- internal standard were numerically removed.

is easily assigned to the vinyl–heme stretching vibration $\nu(C_b\text{–}C_\alpha)$, a ν_{44}-like mode[30] in the reduced symmetry of the ferric protoporphyrin IX ring. The 1125-cm^{-1} vinyl–heme stretch shows an increasing intensity as the excitation wavelength decreases to 225 nm in the bis(cyanide) complex. In contrast, although the 1125-cm^{-1} band shows a comparable intensity at 275-nm excitation for the μ-oxo and bis(imidazole) complexes, at least in the μ-oxo complex it does not increase in intensity as the excitation wavelength decreases. The internal intensity standard, $NaClO_4$, gives rise to the 932-cm^{-1} peak and the weak broad band at ca. 1120 cm^{-1}.

The independence of the 1125- and the 1622-cm^{-1} band frequencies from the identity of bound ligands and the lack of a frequency dependence upon the resulting iron spin state is exactly the behavior previously characterized for the vinyl stretching modes with visible-wavelength excitation.[16] The observed but weak ca. 1370-cm^{-1} bands derive from the symmetric ν_4 porphyrin vibration, which is the oxidation-state marker band that is strongly enhanced with Soret excitation.[16] In iron(III) porphyrins, the ν_4 mode usually occurs at 1370–1375 cm^{-1}, while in reduced iron(II) species it appears at 1355–1360 cm^{-1}, a result of increased back-donation of electron density from Fe d_{xz}, d_{yz} to porphyrin π^* molecular orbitals.[16]

The 275-nm bis(cyanide) PP spectra show bands in addition to the 1622-cm^{-1} vinyl stretch, the ca. 1370-cm^{-1} ν_4 band and 1125-cm^{-1} vinyl–heme stretch. These bands occur at 1580, 1501, 1238, 995, and 760 cm^{-1}. The bis(cyanide) 1580-cm^{-1} porphyrin ν_2 band and the 1501-cm^{-1} porphyrin ν_3 band are sensitive to iron spin state and shift to 1560 and 1484 cm^{-1} in the high-spin μ-oxo complex. The weak ca. 990-cm^{-1} band can be assigned to a vinyl CH wag (γ-CH) on the basis of the Soret-excited heme studies

(35) Choi, S.; Spiro, T. G.; Langry, K. C.; Smith, K. M. *J. Am. Chem. Soc.* **1982**, *104*, 4337–4344.
(36) Choi, S.; Spiro, T. G. *J. Am. Chem. Soc.* **1983**, *105*, 3683–3692.
(37) Lee, H.; Kitagawa, T.; Abe, M.; Pandey, R. K.; Leung, H. K.; Smith, K. M. *J. Mol. Struct.* **1986**, *146*, 329–347.
(38) The skeletal porphyrin ring notation C_a, C_b, and C_m is that of: Hoard, J. L. *Science* **1971**, *174*, 1295–1302.
(39) Teraoka, J.; Kitagawa, T. *J. Phys. Chem.* **1980**, *84*, 1928–1935.
(40) Abe, M.; Kitagawa, T.; Kyogoku, Y. *Chem. Lett.* **1976**, 249–252; *J. Chem. Phys.* **1978**, *69*, 4526–4534.
(41) Kitagawa, T.; Abe, M.; Ogoshi, H. *J. Chem. Phys.* **1978**, *69*, 4516–4525.

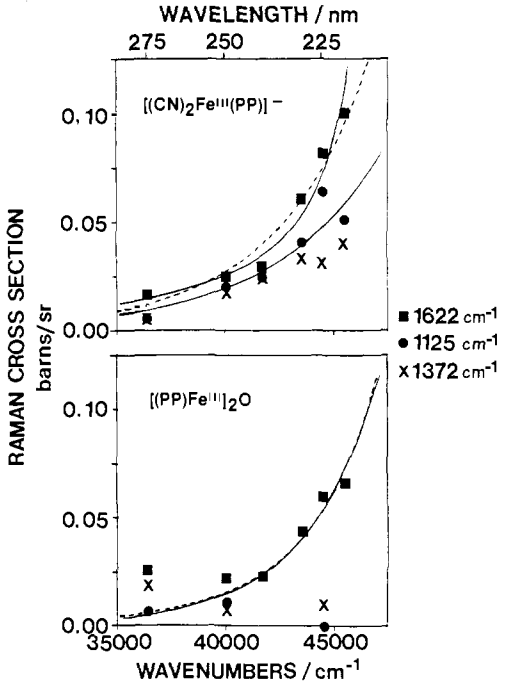

Figure 5. Total differential Raman cross-section excitation profiles for the hemin complexes. Cross sections for the 1622-cm^{-1} vinyl stretch (■), the 1125-cm^{-1} vinyl–heme stretch (●), and the 1372-cm^{-1} porphyrin ν_4 mode (×) are shown. The absolute Raman cross sections for the vinyl mode are *per porphyrin ring* rather than per vinyl group. See Table I for the calculated parameters for the fits to eq 1.

of Choi et al.[30,35] The bis(cyanide) complex shows the presence of a band at ca. 750 cm^{-1} that is most likely the ν_{16} in-plane pyrrole C_aNC_a deformation.[16,36,37] We do not observe enhancement of the vinyl deformation modes at ca. 420 and 330 cm^{-1}, which are observed with Soret excitation.[36,37]

The 250- and 275-nm excited bis(imidazole) hemin spectra show the vinyl and porphyrin bands at 1622 and 1125 cm^{-1}, and at 1372 cm^{-1} with additional relatively weak bands from excess imidazole. In order to assure bis-complexation it was necessary to add a 30-fold excess of imidazole. The Raman spectra of the bis(imidazole) complex with excitation below 250 nm are completely dominated by the enhanced vibrations of the excess imidazole. The vinyl 1622-cm^{-1} peak is discernable, but the imidazole interferences prevent a detailed study of these bands.

For the bis(cyanide) complex we see a selective increase in the Raman cross section for the 1622-cm^{-1} vinyl stretch and the 1125-cm^{-1} vinyl–heme stretch as we excite further into the UV down to 220 nm (see excitation profiles in Figure 5). In contrast, little enhancement is observed for the ca. 1370-cm^{-1} hemin ν_4 mode. In contrast, for the μ-oxo complex, although the 1622-cm^{-1} mode Raman cross section increases with higher energy excitation, the 1125-cm^{-1} band disappears at 225-nm excitation.

Figure 5 displays the 1622-cm^{-1} symmetric vinyl stretch and the 1125-cm^{-1} vinyl–heme stretch excitation profiles measured for bis(cyanide) and μ-oxo dimer hemin complexes in the UV spectral region. These values represent the vinyl mode Raman cross sections *per porphyrin ring*. Of course, protoporphyrin IX contains two vinyl groups on adjacent pyrroles at positions 2 and 4. If the vinyl group motion were strongly coupled, the vibrational modes would occur as pairs involving an in-phase and out-of-phase combination of the respective local modes.[35] We do not, as yet, resolve a clear pair of vibrational modes in either the parallel or perpendicular polarized Raman spectra and assume for the moment that little vibrational coupling occurs. This issue of vinyl coupling has been a source of controversy, which we feel is as yet unresolved, at least for ferric protoporphyrin IX.[35,42]

The μ-oxo excitation profiles show a unique behavior where we observe a decrease in the 1125-cm^{-1} cross section at the shortest excitation wavelengths. However, the almost flat excitation profile for the 1370-cm^{-1} band and the rapid increase in the 1622-cm^{-1} band intensity at higher excitation energy in the μ-oxo complex is similar to that observed for the bis(cyanide) complex. We conclude that the unique μ-oxo excitation profile may result either from the presence of the unique ca. 260-nm strong absorption spectral feature, or from a destructive interference in the 220–250-nm spectral region between a UV transition and the extensively blue-shifted μ-oxo Soret band, or both. Preresonance Soret band enhancement would account for the systematically larger 275-nm Raman cross sections for the μ-oxo complex.

We expect significant enhancement for the 1125-cm^{-1} vinyl–heme stretch by $\pi \rightarrow \pi^*$ porphyrin transitions such as the Soret band because the 1125-cm^{-1} mode involves ca. 50% heme ring motion (analogous to the ν_{44} mode involving C_b–Et and pyrrole C_aC_b stretch in nickel octaethylporphyrin[30,40,41]). Normal mode calculations of Lee et al.[37] indicate a composition of 11% vinyl $C_\alpha C_b$ stretch, 41% vinyl CH_2 motion, and the remainder heme ring stretching.

In the absence of destructive interference we can utilize the A-term preresonance Raman enhancement expression to extract the energy of the excited state that is responsible for the Raman cross section dispersion of the vinyl and porphyrin modes. The A-term model, which gives the intensity dispersion for Franck–Condon active vibrational modes, assumes that a single preresonant excited state, or at most two states, dominate the enhancement. The experimental Raman cross sections σ_A are fit to the A-term frequency dependence given by[21,43]

$$\sigma_A = K_1\nu_0(\nu_0 - \nu_{if})^3\left[\frac{\nu_e^2 + \nu_0^2}{(\nu_e^2 - \nu_0^2)^2} + K_2\right]^2 \qquad (1)$$

where K_1 is a constant proportional to the square of the product of the vibronic matrix elements in the original A-term equation and ν_e is the transition frequency of the excited state responsible for the preresonance enhancement. ν_{if} is the frequency of the vibrational mode and ν_0 is the excitation laser beam frequency in cm^{-1}. The factor $\nu_0(\nu_0 - \nu_{if})^3$ replaces the usual ν_4 dependence term since the photon rate rather than intensity is detected. K_2 is a parameter that allows a second electronic state at higher energy to contribute to the Raman scattering ($K_2 = 0$ for pure A-term dependence where only one electronic state is responsible for the Raman intensity). For example, the modified A-term expression ($K_2 \neq 0$) was required to successfully model enhancement of the vibrational modes of imidazole and acetamide because their enhancement derives from both the nearest $\pi \rightarrow \pi^*$ transition and from other transitions farther in the UV.[17,44]

Figure 5 shows the best fit (by a nonlinear least-squares criterion) to the simple Albrecht A-term (dashed lines) and the modified A-term expression (solid lines). Due to spectral conjection from the imidazole vibrations we were unable to fit the bis(imidazole) data. Because of the complex excitation profile behavior for the μ-oxo complex, we only used the excitation profile data excited at 240 nm and below for the A-term fits. The modified A term models the data better than the simple A term. Table I lists the calculated parameters for the fits. For the 1622-cm^{-1} mode, the preresonant transitions are extrapolated by the modified A term to occur at 201 and 145 nm for the cyanide and μ-oxo dimer, respectively. In contrast, the ν_4 (1372-cm^{-1}) heme ring band shows only a small cross-section dispersion, and an A-term fit does not find a nearby transition.

The data clearly indicate that the vinyl stretching mode at 1622 cm^{-1} of the bis(cyanide) complex is selectively enhanced by an electronic transition that occurs at ca. 200 nm. This behavior is significantly different from that for the heme ring modes (such

(42) Gersonde, K.; Yu, N. T.; Lin, S. H.; Smith, K. M.; Parish, D. W. *Biochemistry* **1989**, *28*, 3960–3966.

(43) Albrecht, A. C.; Hutley, M. C. *J. Chem. Phys.* **1971**, *55*, 4438–4443.

(44) (a) Dudik, J. M.; Johnson, C. R.; Asher, S. A. *J. Phys. Chem.* **1985**, *89*, 3805–3814. (b) Asher, S. A.; Murtaugh, J. L. *Appl. Spectrosc.* **1988**, *42*, 83–90.

Table I. Albrecht A-Term Fits

	simple		modified		
	$K_1/10^{-26}$	ν_e, cm^{-1} (nm)	$K_1/10^{-26}$	$K_2/10^{-8}$	ν_e, cm^{-1} (nm)
bis(cyanide) PP					
1622 cm^{-1}	3.68	70800 (141)	8.64×10^{-4}	3.10	49800 (201)
1125 cm^{-1}[a]	6.09	78500 (127)	6.02	-3.63×10^{-4}	78300 (128)
μ-oxo PP dimer					
1622 cm^{-1}[a]	0.792	63700 (157)	3.31	-1.94×10^{-2}	68900 (145)

[a] Fitted to 240–220-nm data points only.

Table II. Solution Depolarization Ratios ($I_\perp/I_\parallel$) for Ferric Porphyrin Model Complexes and MetMb

	L_2FePP[c]		$Im_2FePPDMe$[d,e]	heme $a^{3+}(Im)_2$[d,e]		MetMb[f]
assignment[a]	457.9[b]	222	406.7	406.7	514.5	430
ν_{10}	0.58 ± 0.04		0.57 ± 0.05	0.28 ± 0.05	0.47	
ν(C=C)	0.42	0.47 ± 0.07	0.43	0.35		0.21 ± 0.02
ν_2	0.38		0.42	0.40	0.40	0.17
ν_3	0.35		0.24	0.20	0.20	0.15
ν_4	0.34		0.30	0.33	0.33	0.14

[a] Assignments based on ref 16; for frequencies for various complexes see Table IV. [b] Wavelength in nm. [c] Data from present study; L = CN^- at 222 nm and L = ImH at 457.9 nm. [d] Data from ref 45 and 46. [e] Im = NMeIm or ImH. [f] Data from ref 47.

as the ca. 1370-cm^{-1} ν_4 band), which are not significantly enhanced by this transition. The 200-nm transition probably derives from the vinyl $\pi \rightarrow \pi^*$ transition, which appears to remain nearly localized on the vinyl group. We do not believe that the value of 145 nm for the modified A-term extrapolated transition for the 1622-cm^{-1} band in the μ-oxo complex is statistically different than the 200-nm value found for the bis(cyanide) complex. This is because we utilized only the few excitation profile data below 240 nm for the fit because of the likely destructive interference present for the longer excitation wavelength profile data, as is evident by the ca. 250-nm excitation profile minimum. We also obtain an extrapolated value of 201 nm if we utilize all of our Raman measurements between 275 and 220 nm. In the bis(cyanide) complex the 1125-cm^{-1} vinyl heme stretch is selectively preresonance enhanced by a UV transition. We tentatively assume that the same transition giving enhancement for the 1622-cm^{-1} mode is responsible for the 1125-cm^{-1} mode preresonance enhancement, but because of additional enhancement from other transitions (especially obvious for the μ-oxo complex) an A-term fit extrapolates a transition energy that is systematically shifted to higher energy from that observed for the 1622-cm^{-1} band.

We measured the depolarization ratio of the vinyl stretching vibration for excitation in the UV at 222 nm and in the visible spectral region in the Soret band (Table II). The easiest comparison is between the Soret measured depolarization ratios for the bis(imidazole) complex (which uniquely shows a well-resolved 1622-cm^{-1} vinyl band) and the UV 222-nm measured depolarization ratio of the bis(cyanide) complex, which shows a well-resolved vinyl band. We observe similar depolarization ratios of ca. 0.45 for the different complexes with both UV and Soret excitation (Table II). It should be noted that most of the data in Table II derives from previously published work. Our measured Soret depolarization ratios agree with measurements by others for similar complexes in aqueous solutions.[45,46] Surprisingly, these values are all significantly larger than those expected for totally symmetric modes of idealized D_{4h} symmetry ($\alpha_{xx} = \alpha_{yy}$, $\alpha_{zz} = 0$), i.e., $\rho = {}^1/_8$. In sharp contrast, however, metmyoglobin depolarization data are close to theoretical expectations based on D_{4h} symmetry.[47]

In order to examine the extent of perturbation of the putative vinyl $\pi \rightarrow \pi^*$ transition by the delocalized heme π orbitals we compared the Raman cross sections of the heme vinyl Raman bands to the C=C stretch in 1-hexene (1641 cm^{-1}) and 1,3-hexadiene (1652 cm^{-1}) dissolved in acetonitrile (Table III). The lowest $\pi \rightarrow \pi^*$ transition of 1-hexene in paraffin[48] occurs at 177 nm and shifts up dramatically to 224 nm in 1,3-hexadiene (in acetonitrile). The resulting resonance Raman cross sections reflect the proximity of the electronic transitions to the 225-nm excitation wavelength. The cross section of the hemin vinyl band is 0.1 barn/sr·molecule, 50-fold higher than that of 1-hexene, but 61-fold smaller than that of 1,3-hexadiene. We conclude that the vinyl attachment to the heme causes a 20-nm red shift of the heme vinyl $\pi \rightarrow \pi^*$ transition. This, along with the observed large depolarization ratio, indicates that some vinyl group conjugation or inductive interactions may occur either in the ground state or in the 200-nm excited state of the protoporphyrin complex.

Table III. Absorption Maxima and Raman Cross Sections for C=C Compounds

compound	$\pi \rightarrow \pi^*$ abs_{max}, nm	Raman cross section[a] ν(C=C), barn/sr·molecule
1-hexene	177[b]	0.002
hemin	ca. 200	0.10
1,3-hexadiene	224[c]	6.1

[a] Laser excitation wavelength, 225 nm. [b] From ref 48; paraffin solution, $\epsilon_{max} \cong 15000$ M^{-1} cm^{-1}. [c] Measured as a 1.74×10^{-4} M solution in acetonitrile, $\epsilon_{max} = 23300$ M^{-1} cm^{-1}.

Our Raman intensities increase linearly with increasing excitation power, and no Raman saturation occurs. Our laboratory previously demonstrated that the measurement of resonance Raman cross sections can be complicated by the occurrence of Raman saturation.[49] With the high incident energy flux of pulsed laser excitation sources, increases in power flux at the sample are often associated with less than a proportional increase in the Raman analyte intensities due to depopulation of the ground state. Jones et al. recently discussed this phenomenon for measurements of pyrene and tyrosinate.[50] While we can force porphyrins to saturate with Soret excitation at high powers, no saturation occurred in the UV Raman spectra discussed here. This robustness of hemes to saturation may derive from their very short lifetimes. Adar et al.[51] calculated heme protein lifetimes from absorption measurements taken in the porphyrin Q absorption band at 77 K and found them to vary between 3 and 100 fs, quite short in relation to our laser pulse width of ca. 6 ns. Based on fluorescence quantum yield studies, open-shell transition-metal porphyrins have lifetimes in the range well below 1 ns; hence, the lack of any

(45) Callahan, P. M.; Babcock, G. T. *Biochemistry* **1981**, *20*, 952–958.
(46) Choi, S.; Lee, J. J.; Wei, Y. H.; Spiro, T. G. *J. Am. Chem. Soc.* **1983**, *105*, 3692–3707.
(47) Sage, J. T.; Morikis, D.; Champion, P. M. *J. Chem. Phys.*, in press.
(48) Robin, M. B. *Higher Excited States of Polyatomic Molecules*; Academic Press: New York, 1975; Vol. II, pp 1–120.
(49) Johnson, C. R.; Ludwig, M.; Asher, S. A. *J. Am. Chem. Soc.* **1986**, *108*, 905–912.
(50) Jones, C. M.; DeVito, V. L.; Harmon, P. A.; Asher, S. A. *Appl. Spectrosc.* **1987**, *41*, 1268–1275.
(51) Adar, F.; Gouterman, M.; Aronowitz, S. *J. Phys. Chem.* **1976**, *80*, 2184–2191.

Table IV. Frequency Dependence of Porphyrin Raman Bands[a,b]

porphyrin	formyl ν(C=O)	ν_{10}	vinyl ν(C=C)	ν_{19}[c]	ν_2	ν_{11}[c]	ν_3	ν_4
$[Fe^{III}PP(ImH)_2]^{+d}$		1640	1620	1586	1579	1562	1502	1373
$Fe^{III}OEP(ImH)_2]^{+d,e}$		1640		1588	1592	1568	1506	1378
Heme $a^{3+}(NMeIm)_2$[f]	1670	1642			1590		1506	1374
$Fe^{II}PP(ImH)_2$[d]		1617	1620	1583	1584	1539	1493	1359
$Fe^{II}OEP(ImH)_2$[e]		1620		1585	1596	1545	1492	1361
Heme $a^{2+}(NMeIm)_2$[f]	1642				1587		1493	1360
$[Fe^{III}PP(DMSO)_2]^{+d,g}$		1610	1621	1560	1559	1545	1480	1370
MetMbF[d,g]		1607	1622	1557	1565	1547	1482	1373

[a] Frequencies in cm^{-1}. [b] Observed with Soret band excitation except where noted. [c] Observed with Q band excitation. [d] From ref 30 and 56. [e] From ref 55. [f] From ref 45 and 56. [g] High-spin complexes; bis(imidazole)porphyrins are low spin.

observable Raman saturation is not surprising.[51,52] We expect even shorter lifetimes for the higher energy transitions due to an increased density of states and the resulting increased relaxation rate.

Discussion

The polarized vinyl C=C stretch at 1622 cm^{-1} was first observed by Spiro and Strekas in Soret-excited Raman spectra of heme proteins,[53] but definitive assignments required extensive C_α and C_β vinyl deuteration studies of NiPP and hemin model complexes.[30,35] Vinyl deformation modes at lower frequency have also been clearly assigned.[35,37] The enhancement of the vinyl modes with visible-wavelength excitation was previously rationalized by assuming conjugation of the vinyl π orbitals with the porphyrin ring. The ca. 10-nm red shift in the Soret and Q bands of protoporphyrins relative to deuterio (H) or meso (CH_3) porphyrins was cited as evidence for this conjugation.[54] Yet, the relative insensitivity of these vinyl stretching frequencies to changes in the porphyrin π-electron density that result from changes in the metal oxidation and spin state suggests little conjugation, at least in the ground state. Table IV summarizes the frequency dependencies of several established porphyrin vibrational modes for different oxidation and spin states. For example, the ν_4 frequency reflects the ring electron density and is diagnostic of metal oxidation state.[16] The ν_{10} frequency is sensitive to the iron coordination number in ferric high-spin complexes.[16] The most striking feature in Table IV is the marked difference between the frequency dependence of the formyl ν(C=O) stretch of heme *a* porphyrins (which contain both vinyl and formyl groups) and the frequency dependence of the vinyl stretch in protoporphyrin IX. The ν(C=O) vibration shifts 28 cm^{-1} to lower frequency between ferric and ferrous forms, while the ν(C=C) frequency in PP remains essentially constant.[30,45,46] This is clear evidence that in the ground state the formyl group must be conjugated to the ring, whereas the vinyls are much less conjugated. Our conclusion of little ground-state vinyl conjugation with the heme π network is supported by the recent theoretical study of Findsen et al.[15] that concluded that little vinyl conjugation was present in the heme ground electronic state.

In the absence of ground-state conjugation, the Soret enhancement of the vinyl vibration suggests excited-state conjugation. In resonance Raman spectroscopy, selective enhancement occurs for those vibrational modes that have their normal coordinate displacements along similar coordinates as the excited electronic state distortion. Hence, resonance enhancement is related to the magnitude of the projection of the vibrational state motion upon the electronic state distortion. Previous workers concluded that the enhancement of the 1622-cm^{-1} band derived from the distortion in the Soret excited state by a "vibrational coupling mechanism".[30] Alternately, the vinyl mode enhancement requires some degree of conjugation with the porphyrin ring in either the ground or excited state.

The intensity of a Raman band increases with the fourth power of the scattered frequency and with the square of the polarizability tensor component $\alpha_{\rho\sigma}$ (ρ,σ = x, y, and z). Under resonance conditions the Raman polarizability tensor may be expressed by the Kramers–Heisenberg–Dirac (KHD) dispersion equation in which the antiresonance term is dropped:[57,58]

$$\alpha_{\rho\sigma} = \sum_{ev} \frac{\langle gf|R_\rho|ev\rangle\langle ev|R_\sigma|gi\rangle}{E_{ev} - E_{gi} - E_0 - i\Gamma} \tag{2}$$

where $\langle gi|$ and $|gf\rangle$ refer to the ground electronic state in vibrational states i and f, respectively, and $|ev\rangle$ represents the vibrational level v in the excited electronic state e. $E_{ev} - E_{gi}$ is the transition energy from the initial ground-state level $|gi\rangle$ to the excited state level $|ev\rangle$. R_σ is the σth component of the electronic dipole moment operator and Γ is the homogenous damping constant, which is proportional to the reciprocal of the excited-state dephasing time. For resonance excitation, by applying the adiabatic approximation and expanding the electronic wave functions in a Taylor series in nuclear displacements according to the Herzberg–Teller formalism, the KHD equation may be expressed in a form that explicitly indicates the major criteria for vibrational resonance enhancement in strongly allowed electronic transitions.[58,59]

$$\alpha_{\rho\sigma} = M^2 \sum_v \frac{\langle f|v\rangle\langle v|i\rangle}{E_v - E_i + E_e - E_0 - i\Gamma} \tag{3}$$

where M is the electronic transition moment matrix element, e.g., $\langle e|R_\sigma|g\rangle$ for the electronic transition to the excited state e. E_e is the 0–0 transition energy from the ground-state zero-vibrational level to the lowest vibrational level of the excited state e. Since resonance enhancement requires $\langle f_1|v_1\rangle\langle v_1|i_1\rangle \neq 0$, Raman scattering occurs only for those symmetric normal modes whose motion occurs along coordinates in which the ground-state equilibrium shifts toward that of the excited state.

If the ground- and excited-state potential surfaces are harmonic and differ only in their equilibrium position along some normal coordinate of vibration, i.e., the vibrational frequencies and normal coordinates remain identical in both electronic states, then each normal mode may be considered as an independent harmonic oscillator with frequency ν and origin shift Δ along its normal coordinate axis. With such approximations, the multidimensional Franck–Condon factors can be explicitly written as simple products of one-dimensional overlaps over the total range of N vibrational degrees of freedom:[59]

$$\langle f|v\rangle = \prod_{j=1}^{N} \langle f_j|v_j\rangle \tag{4}$$

Thus, the polarizability expression for fundamental Raman scattering $f \leftarrow i$ ($f = i + 1$), for a single Raman-active normal coordinate mode, v_1, in a molecule with N normal modes, (ignoring the dependencies of the electronic dipole moment on nuclear configuration) becomes[59]

(52) Seybold, P. G.; Gouterman, M. *J. Mol. Spectrosc.* **1969**, *31*, 1–13.
(53) Spiro, T. G.; Strekas, T. C. *J. Am. Chem. Soc.* **1974**, *96*, 338–345.
(54) Caughey, W. S.; Deal, R. M.; Weiss, C.; Gouterman, M. *J. Mol. Spectrosc.* **1965**, *16*, 451–463.
(55) Ozaki, Y.; Iriyama, K.; Ogoshi, H.; Ochiai, T.; Kitagawa, T. *J. Phys. Chem.* **1986**, *90*, 6105–6112.
(56) Callahan, P. M.; Babcock, G. T. *Biochemistry* **1983**, *22*, 452–461.
(57) Albrecht, A. C. *J. Chem. Phys.* **1961**, *34*, 1476–1484.
(58) Tang, J.; Albrecht, A. C. In *Raman Spectroscopy, Theory and Practice*; Szymanski, H. A., Ed.; Plenum Press: New York, 1970; Vol. II, pp 33–68.
(59) Myers, A. B.; Mathies, R. A. In *Biological Applications of Raman Spectroscopy*; Spiro, T. G., Ed.; John Wiley and Sons, Inc.: New York, 1987; Vol. 2, pp 1–58.

$$\alpha_{i\to f} = M^2 \sum_{v_1=1}^{\infty}\sum_{v_2=1}^{\infty}\sum_{v_N=1}^{\infty} \frac{\langle f_1|v_1\rangle\langle v_1|i_1\rangle \prod_{j=2}^{N}\langle i_j|v_j\rangle\langle v_j|i_j\rangle}{\sum_{j=1}^{N} E_i(v_j - i_j) + E_e - E_0 - i\Gamma} \quad (5)$$

In order to quantitatively relate the magnitude of vibrational mode enhancement to the excited-state distortion it is necessary to relate the normal mode coordinates, Q_j, to a convenient set of internal coordinates, r_k, which are particular bond-stretching and angle-bending motions. This well-known relationship can be written[59]

$$Q_j = \sum_k L_{kj}^{-1} r_k \quad (6)$$

where L_{kj}^{-1} are the matrix coefficients of the normal mode transformation matrix, The total excited-state geometric distortion, Δ_j along a vibrational normal coordinate Q_j is expressible in terms of expansions or contractions along these internal coordinates, δ_k:[59]

$$\Delta_j = \sum_k L_{kj}^{-1}\delta_k \quad (7)$$

The relative L_{kj}^{-1} parameters can be directly obtained from normal mode calculations from the potential energy distribution (PED) of the internal coordinate contributions. The potential energy varies as the square of the vibrational displacement and also depends upon the atomic mass of the nuclei and the normal mode frequency. Thus, the potential energy distribution of internal coordinate motion k in vibrational mode j is proportional to

$$P_{kj} \propto [L_{kj}^{-1}]^2 \quad (8)$$

Although L_{kj}^{-1} is directly proportional to the square root of P_{kj}, the relative signs or phases of L_{kj}^{-1} (along with the signs of Δ_j) often are not readily available.[60]

The excited-state displacements may be related to the Franck–Condon factors for fundamental Raman scattering through the relationship[61]

$$\langle 1|v\rangle_j\langle v|0\rangle_j = \frac{\Delta_j^{2v+1} - 2v\Delta_j^{2v-1}}{2^v 2^{1/2} v!} e^{-\Delta_j^2/2} \quad (9a)$$

In the case of *exact resonance* with a sharp 0–0 transition and in the limit of a very small origin shift ($\Delta_j \to 0$), the important Franck–Condon factors become proportional to the excited-state origin shift along the normal coordinate j:

$$\langle 1|0\rangle_j\langle 0|0\rangle_j \cong \frac{\Delta_j}{2^{1/2}} \quad (9b)$$

We may express the Franck–Condon factors in terms of the potential energy distribution through eq 7 and 8 as

$$[\langle 1|0\rangle\langle 0|0\rangle]_j \propto \sum_k (P_{kj})^{1/2}\delta_k \quad (10)$$

We further assume the absence of Duschinsky rotations in the excited state and we neglect the interaction terms between different internal coordinates.

We can use this approximate expression to examine the degree of enhancement expected for the vinyl stretching vibration since it can be easily partitioned into a component of heme ring stretching r_H and a component of vinyl carbon stretching, r_v:[37]

$$Q_{1622\,cm^{-1}} = L_H^{-1} r_H + L_v^{-1} r_v \quad (11)$$

In the case of *exact resonance* with a sharp 0–0 transition, the polarizability expression for a fundamental Raman band simplifies to

$$\alpha_{i\to f} \propto \frac{-M^2}{i\Gamma}[(P_H)^{1/2}\delta_H + (P_v)^{1/2}\delta_v] \quad (12)$$

We can use this expression to estimate the relative enhancement ratio for the vinyl stretching vibration for excitation within the vinyl $\pi \to \pi^*$ transition and the porphyrin Soret band, This estimate must be approximate because for hemes the homogeneous line width is comparable to the vibrational spacings in both the Soret band and the vinyl transition, This should result, however, in similar relative errors for these transitions and our estimate of the maximum Raman cross sections from eq 12 is likely to be at least qualitatively correct.

The Raman cross-section ratio for the 1622-cm^{-1} vinyl mode excited in the Soret band (B) relative to the ca, 200-nm UV vinyl transition (π) becomes

$$\frac{{}^{v}\sigma^{B}}{{}^{v}\sigma^{\pi}} \cong \left(\frac{\nu_0{}^{B}}{\nu_0{}^{\pi}}\right)\left(\frac{{}^{v}\nu_s{}^{B}}{{}^{v}\nu_s{}^{\pi}}\right)^3\left(\frac{M_B{}^4\Gamma_\pi{}^2}{M_\pi{}^4\Gamma_B{}^2}\right) \times \left[\frac{({}^{v}P_H)^{1/2}\,{}^{v}\delta_H{}^{B} + ({}^{v}P_v)^{1/2}\,{}^{v}\delta_v{}^{B}}{({}^{v}P_H)^{1/2}\,{}^{v}\delta_H{}^{\pi} + ({}^{v}P_v)^{1/2}\,{}^{v}\delta_v{}^{\pi}}\right]^2 \quad (13)$$

where the left-hand superscript v or H signifies either the vinyl vibration or a heme vibration, respectively. This ratio varies as the fourth power of the scattered light frequency and the transition moment matrix elements, and as the inverse square of the homogeneous line widths.

The Raman cross-section ratio for a vinyl vibration relative to a pure heme ring vibration within a single Raman spectrum excited either in the Soret band or in the vinyl 200-nm transition is

$$\frac{{}^{v}\sigma}{{}^{H}\sigma} \cong \left(\frac{{}^{v}\nu_s}{{}^{H}\nu_s}\right)^3\left[\frac{({}^{v}P_H)^{1/2}\,{}^{v}\delta_H + ({}^{v}P_v)^{1/2}\,{}^{v}\delta_v}{({}^{H}P_H)^{1/2}\,{}^{H}\delta_H}\right]^2 \quad (14)$$

where we include the simplification that the coordinate of heme motion in the 1622-cm^{-1} mode and the pure heme mode (e.g., the 1372-cm^{-1} ν_4 mode) are similar (i.e., ${}^{H}\delta_H \equiv {}^{v}\delta_H$).

Equations 13 and 14 give us three independent equations that relate Raman cross-section ratios to heme and vinyl coordinate displacements. These three equations involve the relative Raman cross-section ratios of the vinyl mode and the porphyrin ν_4 mode in the Soret band, as well as in the UV transition and the relative Raman cross-section ratio for the 1622-cm^{-1} vinyl mode between the Soret and the UV transition. We assume that $\Gamma_B = \Gamma_\pi$ and that $M^2 \sim \epsilon$, the molar absorptivity. For the bis(cyanide) hemin, $\epsilon_{Soret} \cong 4\epsilon_{vinyl}$, where we estimate the ϵ_{vinyl} as ca. 20 000 M^{-1} cm^{-1} from the absorption difference between the hemin complexes and gas-phase Fe(OEP)Cl.[26] The observed cross-section ratios are $({}^{v}\sigma/{}^{H}\sigma)^{B} = 0.20$ and $({}^{v}\sigma/{}^{H}\sigma)^{\pi} = 5.0$. Lee and co-workers have calculated the PED for the vinyl vibrational stretching mode at 1631 cm^{-1} in NiPP, which yields contributions of 57% ν(C=C), 26% ν(C$_\alpha$—C$_b$), and 17% derives from motion of the heme ring.[37] C$_\alpha$ is the vinyl carbon attached to the prophyrin ring. We explicitly partition the C$_\alpha$–C$_b$ potential energy equally to the vinyl and heme Franck–Condon factors, $P_v = 0,7$ and $P_H = 0.3$. This partitioning is reasonable since for the bis(cyanide) complex we find that the 1125-cm^{-1} vinyl–ring stretching mode has a Raman cross section with UV excitation intermediate between the 1622-cm^{-1} vinyl stretching mode and the ν_4 mode. Further, we expect that C$_\alpha$–C$_b$ stretching motion will derive enhancement from both the vinyl $\pi \to \pi^*$ transition and the Soret porphyrin ring transition; Soret enhancement has recently been demonstrated for vibrations of aliphatic peripheral ring substituents against the porphyrin ring.[30]

Since the relative signs of the L_{kj}^{-1} values are unknown, we calculate four solutions each for the ratio of displacements in the Soret and UV vinyl $\pi \to \pi^*$ transitions.

$$({}^{v}\delta_v/{}^{H}\delta_H)^{B} = \pm 0.11, \pm 1.2 \text{ and } ({}^{v}\delta_v/{}^{H}\delta_H)^{\pi} = \pm 3.3, \pm 2.0$$

Obviously, the values of ± 1.2 are artifactual since they require that the Soret transition be domainted by vinyl coordinate displacement, which is completely inconsistent with the relatively small perturbation of the porphyrin ring Soret transition upon vinyl group substitution.

We can use the remaining calculated values and eq 13 to compare the relative equlibrium geometry shifts for the vinyl and porphyrin groups upon Soret and vinyl UV $\pi \to \pi^*$ transitions.

(60) Peticolas, W. L.; Blazej, D. C. *Chem. Phys. Lett.* **1979**, *63*, 604–608.
(61) Inagaki, F.; Tasumi, M.; Miyazawa, T. *J. Mol. Spectrosc.* **1974**, *50*, 286–303.

We estimate ${}^{\nu}\sigma^{B}/{}^{\nu}\sigma^{\pi} = 5$ for the ratio of observed vinyl mode Raman cross sections between Soret and UV vinyl $\pi \rightarrow \pi^*$ excitation. We calculated this number based on the measured[62] peak cross section for the ν_4 mode of deoxyMb of ca. 4 barn/sr and from our measured cross sections at 457.9 nm for the ν_4 and vinyl stretch of the bis(imidazole) hemin adduct of 0.16 and 0.03 barn/sr, respectively. Therefore, assuming an excitation profile for the vinyl mode similar to that for the ν_4 mode we estimate a maximum cross section for the vinyl mode in the Soret band to be 1 barn/sr. With a vinyl UV cross section of 0.2 barn/sr we determine that ${}^{\nu}\sigma^{B}/{}^{\nu}\sigma^{\pi} = 5$. Thus, we obtain ratios for the vinyl coordinate distortions, ${}^{\nu}\delta_{\nu}^{B}/{}^{\nu}\delta_{\nu}^{\pi}$ between 0.21 and 0.60. This range of values indicates a significantly smaller shift along the vinyl coordinate for Soret band excitation compared to UV excitation. In contrast, we obtain ratios for ${}^{\nu}\delta_{H}^{B}/{}^{\nu}\delta_{H}^{\pi}$ between 3.94 and 16.2, and this range of values indicates a much larger shift for the heme coordinate of the vinyl vibration with Soret excitation compared to excitation within the UV vinyl $\pi \rightarrow \pi^*$ transition.

Enhancement of the vinyl vibration within the Soret band could derive simply from the fact that the vinyl vibrational mode contains ca. 17% heme motion, or it could derive from the conjugation of the vinyl orbitals with the heme orbitals and the resulting spatial expansion of the Soret transition into the vinyl substituents. The values of the calculated results here clearly demonstrate that the enhancement of the vinyl mode in the Soret electronic transition derives from conjugation of the Soret π orbitals into the vinyl orbitals, which results in a vinyl coordinate displacement in the Soret excited state; however, the relative vinyl coordinate displacement in the Soret band is significantly smaller than the heme coordinate displacement. Similarly, these results indicate a small but significant heme conjugation with the UV vinyl excited state. Thus, the vinyl mode enhancement by the Soret transition and the heme mode enhancement by the UV vinyl transition are the direct result of conjugation between the respective π orbitals.

The vinyl group distortion that occurs with Soret excitation indicates that conjugation occurs between the vinyl π or π^* frontier orbitals and the heme π or π^* orbitals. From the theoretical calculations of Findsen et al.[15] discussed above, which show negligible ground-state conjugation and the lack of frequency sensitivity of the vinyl modes to iron coordination, spin state, and ligation, we conclude that the conjugation must take place in the Soret excited state. This would be consistent with electron density calculations[1] of porphyrins, which show significant electron density at adjacent C_b sites of pyrroles in the excited e_g (LUMO) porphyrin state, while little or no C_b pyrrole electron density occurs in the ground-state occupied a_{1u}, a_{2u} porphyrin HOMOs; electron density at C_b allows easy mixing of the vinyl and heme orbitals.

If the excited-state coordinate displacement were associated with bond order changes associated with transfer of electron density between π and π^* orbitals, the Soret transition calculated value of $({}^{\nu}\delta_{\nu}/{}^{H}\delta_{H})^{B} = 0.1$ would have ca. 90% of the electron displacement occur within the π^* orbital of the heme ring and only 10% of the electron displacement transfer into the π^* orbitals of the vinyl groups. In contrast, when exciting in the UV, the $({}^{\nu}\delta_{\nu}/{}^{H}\delta_{H})^{\pi}$ ratio of 2.0 or 3.3 indicates that between 67% and 77% of the electron motion occurs within the vinyl π^* orbitals and only 23% and 33% of the electron motion transfers into the heme ring π^* orbitals. Thus, we conclude that there is modest vinyl–heme orbital conjugation in the Soret excited state. Although a small amount of conjugation or orbital mixing with the heme is evident for the ca. 200-nm UV transition, it is mainly an isolated vinyl $\pi \rightarrow \pi^*$ electronic excitation. It should also be noted that the calculated values of ${}^{\nu}\delta_{\nu}^{B}/{}^{\nu}\delta_{\nu}^{\pi} = 0.21$–$0.60$ and ${}^{\nu}\delta_{H}^{B}/{}^{\nu}\delta_{H}^{\pi} = 3.94$–$16.2$ independently indicate the domination of the ca. 200-nm transition by the vinyl group and the domination of the Soret band by the heme macrocycle.

A number of cautionary statements are required to qualify our analysis. We have not actually measured the maximum Raman cross section of the vinyl mode under exact resonance in either the Soret band or the UV transition. Thus, we have a lower bound estimate of the relative C=C displacements for these resonances. It is therefore possible that there may be somewhat greater vinyl involvement in the visible Soret transition and even less porphyrin involvement in the 200-nm transition than we calculate. In addition, we assume similar values of the homogeneous line width for the two transitions. This could cause an error in our calculation that would scale with the square of the relative homogeneous line widths.

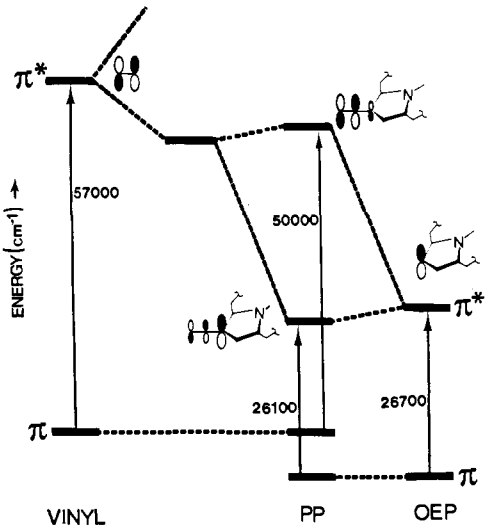

Figure 6. Qualitative energy level diagram showing mixing of the vinyl π^* antibonding molecular orbital with the Soret porphyrin π^* molecular orbital. The porphyrin orbital localized on the C_b pyrrole, which is bonded to a vinyl group, is shown. No mixing occurs in the ground state. See text for details.

Our conclusion of excited-state vinyl group conjugation with the porphyrin excited Soret state is illustrated in the qualitative orbital energy diagram shown in Figure 6. There is no mixing in the ground state between the occupied orbitals of the vinyl group and the porphyrin ring. Our data suggest that a small amount of conjugation exists in the excited states. The molecular orbital diagram displays the observed Soret band red shift associated with protoporphyrins compared with OEP. Further, our results indicate small vinyl–heme molecular orbital mixing in the ca. 200-nm transition and the presence of an almost isolated vinyl transition. The vinyl $\pi \rightarrow \pi^*$ transition also shows a red shift in energy, which in a simple two-level LCAO–MO scheme is impossible. Obviously, we must have a more complex situation that reflects the high density of porphyrin states present in the 200-nm UV spectral region. The effect of a potentially large number of interactions with these higher energy porphyrin states is a net stabilization of the vinyl π^* orbital. In fact, in addition to the numerous underlying porphyrin UV $\pi \rightarrow \pi^*$ transitions that give rise to strong absorption in porphyrins everywhere in the UV, we have the well-known complexity of the various postulated orbital excitations associated with the vinyl first "singlet $\pi \rightarrow \pi^*$ transition".[63]

While some controversy still exists, the consensus is that the first allowed ethylenic transition involves a transition to a mixed state of $\pi \rightarrow \pi^*$, Rydberg, and $\sigma \rightarrow \sigma^*$ character. In fact, this excited state in ethylene is twisted 90° about the C–C bond relative to the ground state.[63,64] A similar mixing of π^* and σ^* orbitals should occur for the analogous vinylic transition in olefins. In our case, the π^* component should preferentially mix with the Soret e_g excited orbital. Geometrically then, we expect a planar π system for the Soret excited state. However, the ca. 200-nm higher energy transition is not constrained to maintain planar vinyl groups relative to the heme.

(62) Bangcharoenpaurpong, O.; Schomacker, K. T.; Champion, P. M. *J. Am. Chem. Soc.* **1984**, *106*, 5688–5698.

(63) Robin, M. B. *Higher Excited States of Polyatomic Molecules*; Academic Press: New York, 1985; Vol. III, pp 213–236.

(64) Ziegler, L. D.; Hudson, B. S. *J. Chem. Phys.* **1983**, *79*, 1197–1202.

The lack of conjugation between the vinyl and the porphyrin ring in the ground state is consistent with the heme structure as probed by X-ray crystallography, Little et al,[13] demonstrated that the 1-methylimidazole Fe(III) porphyrin complex $[(1\text{-MeIm})_2Fe(PP)]^+$ has a significantly ruffled core with the two vinyl groups rotated out of the pyrrole planes by 24 and 41°. If the vinyls were strongly conjugated they would remain coplanar. Caughey and Ibers[14] also found that the vinyl groups of free base protoporphyrin IX dimethyl ester were not coplanar with the pyrroles. They attributed this lack of planarity as due to steric restraints, between an H_β on the vinyl and the H atoms of adjacent methyl groups, as well as steric interactions between the vinyl H_α and the proximate methine H atom.

It is interesting that the diffuse broad porphyrin $\pi \rightarrow \pi^*$ UV transitions do not give significant resonance enhancement of porphyrin modes, This lack of enhancement probably derives from the large homogeneous line widths that give these transitions such diffuse character.

The large depolarization ratios listed in Table II indicate significant deviations from D_{4h} symmetry for our cyanide complex as well as for similar complexes previously studied by other workers. In fact, the depolarization ratios most consistent with a D_{4h} symmetry were measured for myoglobin.[47] The large depolarization ratios for the heme ring vibrations obviously indicate breaking of the in-plane x,y degeneracy and a mixing in of nominally B_{1g} or B_{2g} character into the A_{1g} vibrational modes.[35,45,65,66] On the other hand, the large depolarization ratio of 0.47 measured for the vinyl mode with UV excitation may not be anomalous, since the depolarization ratio of 1,3-hexadiene with 222-nm excitation is 0.45. Although the depolarization ratio should be 0.33 for the vinylic single C=C transition, the larger depolarization ratio is indicative of additional tensor component contributions, Furthermore, the analysis of the depolarization ratio for the two vinyl groups in protoporphyrin IX is complex since it intimately depends upon whether the two vinyl vibrations are coupled. We are presently examining this question.

(65) Collins, D. W.; Fitchen, D. B.; Lewis, A. *J. Chem. Phys.* **1973**, *59*, 5714-5719.
(66) Nafie, L. A.; Pezolet, M.; Peticolas, W. L. *Chem. Phys. Lett.* **1973**, *20*, 563-568.

Conclusions

Our conclusion that there is little conjugation between the vinyl groups and the porphyrin ring in the ground state is suggestive that the vinyl groups have little role in controlling heme reactivity. However, proteins may be able to exercise control on heme reactivity to the extent that the protein perturbation mixes excited-state frontier orbitals of the heme into the ground-state occupied orbitals. For example, the protein could force the vinyl groups to lie planar, and this might mix the vinyl orbitals with the heme orbitals within the ground state. This effect may not be calculable by the techniques of Findsen et al.[15] In fact, recently Gersonde et al.[42] demonstrated that the vinyl groups in the heme of an insect hemoglobin are so perturbed by the surrounding protein that the two vinyl stretching frequencies split by 7 cm^{-1}.

An obvious conclusion from our study is that one can directly monitor the magnitude of protein–vinyl group interactions by measuring the Soret band enhancement of the vinyl stretching modes. The vinyl mode Soret cross section is directly related to the extent of conjugation. We are in the process of measuring these cross sections in a series of heme proteins,

Acknowledgment. We thank Professor Ken Jordan for many helpful conversations and gratefully acknowledge support of this work from NIH Grant 1R01GM30741-08, Sanford A. Asher is an Established Investigator of the American Heart Association. This work was done during the tenure of an Established Investigatorship of the American Heart Association, Pennsylvania affiliate.

Thermochemical Properties of Gas-Phase MgOH and MgO Determined by Fourier Transform Mass Spectrometry

Lorenza Operti,[†] Edward C, Tews,[‡] Timothy J. MacMahon, and Ben S, Freiser*

Contribution from the Department of Chemistry, Purdue University, West Lafayette, Indiana 47907. *Received December 23, 1988*

Abstract: Gas-phase thermochemical values $D°(Mg^+–OH)$ = 75 ± 4 kcal/mol, IP(MgOH) = 7.3 ± 0.1 eV, $D°(Mg^+–O)$ = 53 ± 3 kcal/mol, and IP(MgO) = 7.9 ± 0.1 eV have been experimentally determined by photodissociation measurements and charge-transfer reactions with Fourier transform mass spectrometry. These results, together with previously determined thermochemical data, are used to determine other thermochemical properties of MgOH and MgO. Our value $D°(Mg–OH)$ = 67 ± 6 kcal/mol agrees well with previous experimental values. However, $D°(Mg–O)$ = 59 ± 5 kcal/mol is much lower than previous experimental results, which vary widely, but is in good agreement with a recent ab initio CI calculation.

The thermochemical properties of gas-phase metal monohydroxides have recently been of interest due to the roles these species play in flame chemistry[1] and meteor ablation processes.[2] Most of the bond dissociation energies of the neutral species have come from flame measurements.[3] More recent measurements from Knudsen cell mass spectrometry,[4-6] however, have indicated that some of the results reported earlier may be high by as much as 15 kcal/mol.[5] Consequently, this study was undertaken to yield another independent measurement of the bond dissociation energy of Mg–OH. Direct measurements were obtained for $D°(Mg^+–$

* Author to whom correspondence should be sent.
[†] Present address: Istituto di Chimica Generale ed Inorganica, Universitá di Torino, Torino, Italy.
[‡] Present address: Abbott Laboratories, Bldg. R1B, Dept. 48T, N. Chicago, IL 60064.

(1) Hastie, J. W. *High Temperature Vapors-Science and Technology*; Academic: New York, 1975.
(2) (a) Murad, E.; Swider, W. *Geophys. Res. Lett.* **1979**, *6*, 929. (b) Murad, E.; Swider, W.; Benson, S. W. *Nature* **1981**, *289*, 273.
(3) (a) JANAF Thermochemical Tables. *J. Phys. Chem. Ref. Data* **1978**, *7*, 793. (b) Gurvich, L. V.; Ryabova, V. G.; Khitrov, A. N. *Faraday Symp. Chem. Soc.* **1973**, *8*, 83.
(4) Murad, E. *J. Chem. Phys.* **1981**, *75*, 4080.
(5) Murad, E. *Chem. Phys. Lett.* **1980**, *72*, 295.
(6) Murad, E. *J. Chem. Phys.* **1980**, *73*, 1381.

0002-7863/89/1511-9152$01.50/0